

## Conclusions

In the vicinity of the wall surface, mixing between the coolant and the primary fluid was unimportant, and the coolant layer produced effective film cooling in the region of shock wave/film cooling interaction. Viscous effects on momentum transfer were small in the region of interaction. Based on this result, a flow structure model was constructed to simulate the pressure distribution. It was possible to predict the separation of the film coolant using the calculated pressure distribution and a formula for a subsonic, turbulent boundary layer.

## References

- <sup>1</sup>Kanda, T., Ono, F., Takahashi, M., Saito, T., and Wakamatsu, Y., "Experimental Studies of Supersonic Film Cooling with Shock Wave Interaction," *AIAA Journal*, Vol. 34, No. 2, 1996, pp. 265–271.
- <sup>2</sup>Kanda, T., Ono, F., and Saito, T., "Experimental Studies of Supersonic Film Cooling with Shock Wave Interaction," *AIAA Paper* 96-2663, July 1996.
- <sup>3</sup>Kwok, F. T., Andrew, P. L., Ng, W. F., and Schetz, J. A., "Experimental Investigation of a Supersonic Shear Layer with Slot Injection of Helium," *AIAA Journal*, Vol. 29, No. 9, 1991, pp. 1426–1435.
- <sup>4</sup>Hyde, C. R., Smith, B. R., Schetz, J. A., and Walker, D. A., "Turbulence Measurements for Heated Gas Slot Injection in Supersonic Flow," *AIAA Journal*, Vol. 28, No. 9, 1990, pp. 1605–1614.
- <sup>5</sup>Bass, R., Hardin, L., Rodgers, R., and Ernst, R., "Supersonic Film Cooling," *AIAA Paper* 90-5239, Oct. 1990.
- <sup>6</sup>Juhany, K., and Hunt, M. L., "Flowfield Measurements in Supersonic Film Cooling Including the Effect of Shock-Wave Interaction," *AIAA Journal*, Vol. 32, No. 3, 1994, pp. 578–585.
- <sup>7</sup>White, F. M., *Viscous Fluid Flow*, McGraw-Hill, New York, 1974, pp. 522–529.

## View Factors for Rectangular Enclosures Using the Direct Discrete-Ordinates Method

K. H. Byun\*

Dongguk University, Seoul 100-715, Republic of Korea  
and

Theodore F. Smith†

University of Iowa, Iowa City, Iowa 52242-1527

## Introduction

VIEW factor results for various geometries appear frequently in the literature and can be calculated by several methods.<sup>1,2</sup> The speed, accuracy, and unique characteristics of several different numerical methods are compared in Ref. 3. Sanchez and Smith<sup>4</sup> proposed that view factors be calculated by using the discrete-ordinates method (DOM). The DOM is applied to compute view factors for an infinite rectangular geometry enclosing a transparent medium.<sup>5</sup> Ehlert and Smith<sup>6</sup> apply the DOM to compute the radiant exchange for a three-dimensional rectangular enclosure. A quadrature set based on equal weights and satisfying odd moments was used for the results. Byun<sup>7</sup> computed view factors for a rectangular box using the DOM. The weights and directions are based on the spatial divisions on the boundary surfaces.

The purpose of this study is to compute view factors for a rectangular box enclosing a transparent medium by using the

direct DOM ( $DS_N$ ). The word direct is used to imply that the weights and directions are derived using spherical coordinates. A protrusion may exist in the black wall enclosure.

## Analysis

The system under study is shown in Fig. 1 with the coordinate system. It is assumed that the heat transfer occurs only by thermal radiation. The length, width, and height of the enclosure are  $L$ ,  $W$ , and  $H$ , respectively. The protrusion length is denoted as  $L_1$ , the width as  $W_1$ , and the height as  $H_1$ . The rectangular box-type control volumes are generated by dividing the length, width, and height of the system by  $n_j$ ,  $n_i$ , and  $n_k$ , respectively. Subscripts  $T$ ,  $B$ ,  $N$ ,  $S$ ,  $E$ , and  $W$  refer to the top, bottom, north, south, east, and west surfaces, respectively. A positive superscript (+) is assigned for the intensity leaving the control volume, whereas a negative superscript (−) for entering the control volume.

The radiative transport equation<sup>1,2</sup> for an arbitrary  $i$ th direction is discretized by using the intensity at point  $P$  and the intensities at the west and south boundaries. This results in

$$I_{iP}^+ = \frac{\mu_i I_{iW}^- + \eta_i I_{iS}^- + \xi_i I_{iB}^-}{\mu_i + \eta_i + \xi_i} \quad (1)$$

when the control volume shape is a cube.  $I$  is the intensity, and  $\mu_i$ ,  $\eta_i$ , and  $\xi_i$  are  $x$ -,  $y$ -, and  $z$ -direction cosines, respectively. By employing the same procedure used for deriving Eq. (1), the other intensity expressions can be derived.

If the radiative flux at the east surface is expanded in a Taylor series about the radiative flux at point  $P$ , then

$$q_{iE} = q_{iP} + \frac{\partial q_{iP}}{\partial x} \frac{\Delta x}{2} + \mathcal{O}(\Delta x^2) \quad (2)$$

After discretizing the differential terms in Eq. (2) by  $q_E$  and  $q_w$ , and substituting the radiative flux expressions that are the product of intensity and direction cosines, the result is

$$I_{iE}^+ = I_{iP}^+ + \frac{I_{iE}^- - I_{iW}^-}{2} = 2I_{iP}^+ - I_{iW}^- \quad (3)$$

The intensity expressions at the  $N$ ,  $S$ ,  $W$ ,  $T$ , and  $B$  can be obtained using a similar procedure as described for Eq. (3). Equation (3) is the same as the intensity relations in Refs. 6 and 7 if a value of 0.5 is used for the finite difference weighting factor. The positive intensities at control volume  $P$  become the negative intensities at adjacent control volumes.

For black boundary walls, the radiative intensity of the  $i$ th direction is

$$I_{i,\text{wall}}^+ = \frac{\sigma T_{i,\text{wall}}^4}{\pi} \quad \text{wall} = N, S, E, W, T, B \quad (4)$$

where  $\sigma$  is the Stefan-Boltzmann constant, and  $T$  is the absolute temperature.

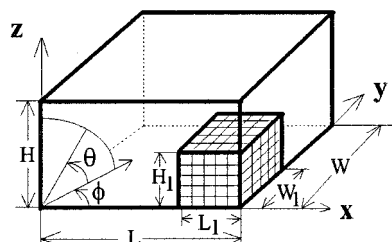


Fig. 1 System description.

Received March 10, 1997; revision received May 20, 1997; accepted for publication May 20, 1997. Copyright © 1997 by the American Institute of Aeronautics and Astronautics, Inc. All rights reserved.

\*Associate Professor, Department of Mechanical Engineering.

†Professor, Department of Mechanical Engineering, Member AIAA.

The radiative fluxes at each boundary surface  $q_{\text{wall}}$  are as follows:

$$q_{\text{wall}} = \sum_{i=1}^{4M} c_i \omega_i (I_i^+ - I_i^-) \quad \text{wall} = E, W, N, S, T, B \quad (5)$$

where  $\omega_i$  is the weighting factor for the  $i$ th direction and  $M$  is the number of directions per octant:  $c_i = \mu_i$  for  $E, W$ , wall,  $c_i = \eta_i$  for  $N, S$  wall, and  $c_i = \xi_i$  for  $T, B$  wall.

### Discrete-Ordinates Parameters

The surface of a sphere of radius one in the first octant is uniformly divided by  $N_\phi$  and  $N_\theta$ , where  $\phi$  is the angle in the  $x$ - $y$  plane measured from the  $x$  axis, and  $\theta$  is the angle measured from the  $x$ - $y$  plane. There are  $M$  segments on the unit sphere in one octant, where  $M = N_\theta N_\phi$ . The discrete-ordinates directions are defined at the center of each segment:

$$\mu_{ij} = \cos \theta_i \cos \phi_j, \quad \eta_{ij} = \cos \theta_i \sin \phi_j, \quad \xi_{ij} = \sin \theta_i \quad (6)$$

Subscripts  $i$  and  $j$  are used for segment center indices.

Because all of the surfaces are diffuse, the discrete-ordinates weights are defined in terms of the solid angles of each segment:

$$\omega_{ij} = \cos \theta_i \Delta \theta \Delta \phi \quad (7)$$

The right-hand side of Eq. (7) is independent of angle  $\phi$  because of the uniform division. As  $N_\theta$  and  $N_\phi$  go to infinity, the sum of the weights in an octant converge to  $\pi/2$ . Also, the sum of the product of  $i$ th direction weight and  $\mu_i$ ,  $\eta_i$ , and  $\xi_i$  in an octant converge to  $\pi/4$ .

The numerical solution procedure is the same as that used for the standard discrete-ordinates solutions procedure.<sup>6,7</sup> To find the view factor from a source surface to a target surface, the source surface is assigned an emissive power of 1, and all other surfaces have zero emissive power. The radiative flux at a surface is the view factor from the source surface to that surface.<sup>4</sup> The view factors from the source surface to all surfaces in the enclosure are obtained simultaneously.

### Results and Discussion

The method described in the analysis is applied to two examples. For the first example, view factors for a cube without

and with a protrusion are computed. The protrusion is located in a cubical enclosure and  $H_1/H = L_1/L = W_1/W = 0.5$ . The view factor from the bottom surface to the top surface,  $F_{B-T}$ , is tabulated in Table 1 by varying the spatial division  $n$  and angular division in one octant,  $N = N_\theta = N_\phi$ . The length, width, and heights are each divided by  $n$ . The results without and with a protrusion are in Tables 1a and 1b, respectively. For both cases, the symmetry conditions, enclosure relation,<sup>1,2</sup> and the reciprocity relations<sup>1,2</sup> are examined and confirmed.

The results for no protrusion show the following tendency. For  $n \geq 16$  and  $N \geq 16$ , the relative error with respect to the exact value is less than  $\pm 1\%$ . At a fixed spatial division, increasing  $N$  up to  $n$  shows the tendency of improving the accuracy. Further increasing  $N$  beyond  $n$  does not improve the accuracy. The absolute error for  $n = N = 32$  is approximately 0.0002, and for  $n = N = 64$  it is approximately 0.00005. Thus, by doubling the spatial divisions, the errors are reduced by a factor of 1/4. To five significant digits, the exact value of  $F_{B-T}$  is 0.19982 (Ref. 6).

The tendencies for the results with a protrusion are as follows. The values of the view factors by  $DS_N$  converge to the accurate values as  $n$  and  $N$  increase. The results indicate that more spatial and angular divisions are needed to improve the accuracy of the results when a protrusion exists. For  $n \geq 64$ , the error compared to the exact value is less than  $\pm 1\%$  for any  $N$ . To four significant digits, the exact value of  $F_{B-T}$  is  $0.1750 \pm 0.0001$ . The view factor relations in Refs. 1 and 2 cannot be applied to this case because of the shading and special care needed to compute the view factors accurately from the integral expressions.

The computations were done on a personal computer with a 80686-166 MHz processor and 32 Mb RAM. The program was compiled using a 32-bit Fortran compiler. About 20 s of computing time is required for the  $n = N = 16$  results and about 5.3 h of computing times are required for  $n = N = 64$  results.

For the second example, view factors for rectangular boxes with different aspect ratios are computed using the  $DS_N$  method; there is no protrusion. The exact values are computed from Ref. 6. The dimension of  $L$ ,  $W$ , and  $H$  are shown in Table 2. The number of spatial divisions for  $H$  is  $n$ , the spatial division for  $L$  is  $n \times (L/H)$ , and the spatial division for  $W$  is  $n \times (W/H)$ . The angular division used for the results is  $N = n$ . Good agreements with the exact values are observed in Table 2. The absolute errors for the long square duct cases are approximately 0.0002 for  $(L/H)$  values from 1 to 10.

### Conclusions

The purpose of this study is to compute the view factors for a three-dimensional rectangular box enclosing a transparent media by using the  $DS_N$  method. The discrete-ordinates weights and directions are derived by spherical coordinates. One of the advantages of the  $DS_N$  method is that the weights and directions can be easily generated and implemented. From the example cases, it is concluded that view factors for the system without protrusion can be accurately obtained by using the  $DS_N$  method. For the system with a protrusion, more refinement of spatial and angular divisions than used in this study are needed to improve the accuracy. The results indicate that the accuracy depends not only on the spatial division, but also on the angular divisions. For a given spatial division  $n$ , significant improvement in the accuracy is found by increasing

Table 1 Effects of  $n$  and  $N$  on view factor  $F_{B-T}$

$n$	$N$			
	8	16	32	64
a) No protrusion case (0.19982, Ref. 6)				
16	0.20314	0.19894	0.19875	0.19866
32	0.20224	0.20064	0.19961	0.19955
64	0.20276	0.20012	0.19998	0.19978
b) With protrusion case (0.1750)				
16 (Ref. 7)	0.1695	0.1702	0.1707	—
	0.1753	0.1712	0.1709	0.1708
32 (Ref. 7)	0.1700	0.1713	0.1718	—
	0.1744	0.1729	0.1719	0.1718
64	0.1761	0.1739	0.1736	0.1735

Table 2 View factor  $F_{B-T}$  for rectangular enclosure by  $DS_N$

$n$	$(L, W, H)$						
	(2, 1, 1)	(4, 1, 1)	(10, 1, 1)	(2, 2, 1)	(3, 3, 1)	(3.5, 3.5, 1)	(3, 2, 1)
32	0.28568	0.34578	0.38619	0.41524	0.54737	0.59396	0.47556
48	0.28583	0.34590	—	0.41524	—	—	—
Exact	0.28588	0.34596	0.38638	0.41525	0.54738	0.59399	0.47558